

Available online at [www.sciencedirect.com](http://www.sciencedirect.com)**ScienceDirect**

Energy Procedia 126 (201709) 770–777

Energy

**Procedia**[www.elsevier.com/locate/procedia](http://www.elsevier.com/locate/procedia)

72<sup>nd</sup> Conference of the Italian Thermal Machines Engineering Association, ATI2017, 6-8  
September 2017, Lecce, Italy

## Experimental and CFD analyses of a highly-loaded gas turbine blade

Tommaso Bacci<sup>a</sup>, Andrea Gamannossi<sup>b\*</sup>, Lorenzo Mazzei<sup>a</sup>, Alessio Picchi<sup>a</sup>, Lorenzo Winchler<sup>a</sup>,  
Carlo Carcasci<sup>a</sup>, Antonio Andreini<sup>a</sup>, Luca Abba<sup>c</sup>, Stefano Vagnoli<sup>c</sup>

<sup>a</sup>Department of Industrial Engineering, University of Florence, Via di S. Marta, 3 – 50139 Firenze – Italy

<sup>b</sup>Department of Engineering and Architecture, University of Parma, Via Università, 12 – 43121 Parma – Italy

<sup>c</sup>Ansaldo Energia, Via N. Lorenzi, 8 – 16152 Genova – Italy

---

### Abstract

The estimation of metal temperature is paramount to ensure an adequate life span of gas turbine hot gas path components. An experimental campaign was carried to investigate pressure loading and metal temperature distribution of an industrial blade cooled by means of straight smooth channels. Changing mainstream and coolant mass flow rates it was thus possible to characterize the thermal response at different operating conditions. CFD simulations allowed to relate the metal temperature distribution to the processes of laminarization and transition of the boundary layer. Further sensitivity analyses aimed at estimating the impact of the uncertainty associated with certain boundary conditions highlighted that a reduction in mainstream turbulence at leading edge of 30% can reduce metal temperature up to 5%, whereas coolant turbulence plays a minor role. The same effect was pointed out when the actual surface roughness of the internal channels was accounted for. Particular attention should be paid to this parameter in the thermal design of additive manufactured components when surface finishing is not feasible.

© 2017 The Authors. Published by Elsevier Ltd.

Peer-review under responsibility of the scientific committee of the 72<sup>nd</sup> Conference of the Italian Thermal Machines Engineering Association

*Keywords:* Gas Turbine; Heat Transfer; Cooling; IR; CFD; CHT; Turbulence; Transition.

---

\* Corresponding author. Tel.: 055 2758771;  
E-mail address: [andrea.gamannossi@studenti.unipr.it](mailto:andrea.gamannossi@studenti.unipr.it)

## 1. Introduction

In order to improve gas turbines performances, in terms of higher thermodynamic efficiency and power output, an increase of Turbine Inlet Temperature (TIT) level is mandatory. Nevertheless, higher TIT values also imply stronger thermal loads on all the engine components exposed to the gas flow: consequently, cooling systems are applied, with the aim to keep components temperature to a level that is compatible with an adequate lifespan but trying to minimize coolant consumptions. An accurate prediction of metal temperatures in a gas turbine component design phase is of paramount importance since deviations of 40-80K at the full power engine condition could potentially result in life predictions that vary by a factor of 10 [1].

Several experimental and numerical works dealing with gas turbine component temperature predictions can be found in literature. Metal temperatures on a gas turbine vane or blade can be evaluated by using different techniques like thermocouples, like in the early works performed by Hylton et al. [2] with Mark II and NASA C3X experimental campaign, naphthalene sublimation or thermochromic liquid crystals (TLC) [3]. In recent years, IR camera technique is used more and more due to its advantages respect to TLC: IR method only requires black paint on the to-be-analyzed surface, it does not require a sophisticated illumination system and it is not bounded by a small operating temperature range. Ekkad et al. [4] used IR technique for film effectiveness and heat transfer measurements, while Lynch and Thole [5] used it for endwall HTC evaluations; Cocchi et al. [6] and Goodro et al. [7] applied IR techniques for a detailed analysis of impingement jets. An extensive review of IR thermography application to heat transfer measurements was performed by Carlomagno and Cardone [8]. In this work, an IR camera was used for directly measuring metal temperatures on a cooled blade, with the goal of studying its behavior in different operating conditions and producing reliable experimental results to be used in numerical validations.

Fully coupled Conjugate Heat Transfer (CHT) simulations are widely used for predicting metal temperatures, since they have the capability to compute heat conduction through solids coupled with the heat convection transferred from fluid flows, removing the uncertainty associated with calculating solid-fluid interface boundary conditions [1]. For brevity, only a few works dealing with CHT are here reported, like the pioneering works of Bohn et al. [9], the turbulence models assessment performed by York and Leylek [10] and Facchini et al. [11], and a comparison between coupled and decoupled approach analysed by Andrei et al. [12]. In the present paper, CHT simulations performed with Fluent are reported and validated with experimental data, in order to have a better comprehension of the complex heat transfer and fluid dynamics phenomena involved.

## 2. Experimental setup

### 2.1. Test article configuration

Measurements have been performed on a prismatic blade model 3D printed in inconel. The test article profile has been built by extruding the midspan profile of a first stage rotor blade with a reduction scale factor of 1.5.

The test article, shown in Fig. 1, has an internal cooling system made of a U-bend smooth channel. The cooling flow is fed from the tip of the blade, as sketched in Fig. 1a, where the bottom part of the blade is reported in transparency in order to have a clear view of the coolant path in correspondence of the bend.

The goal of the measurement campaign is to evaluate the blade metal temperature for different mainstream and coolant conditions by means of IR thermography. In order to calibrate the IR camera output, the blade is provided with 10 thermocouples embedded 0.6 mm beneath the blade external surface. Differences between the measured values and the actual external wall temperatures have been evaluated to stay within 3 K. Besides, 12 pressure taps, clearly visible in Fig. 1, have been distributed at the blade midspan to measure the isentropic Mach number distribution on the profile and get additional information about the mainstream boundary conditions.

The test sample temperature is measured as it is invested by a hot main flow, in order to create realistic conditions both in terms of external heat transfer and mainstream-to-coolant temperature ratio. The test section is sketched in Fig. 1b-c: the casing, where the blade is installed, is made by direct metal laser sintering, and its lateral walls have the same shape of the blade pressure side and suction side to simulate the presence of adjacent blades. A CFD optimization process has been conducted for the design of both the casing and the downstream duct, to recreate periodic conditions.

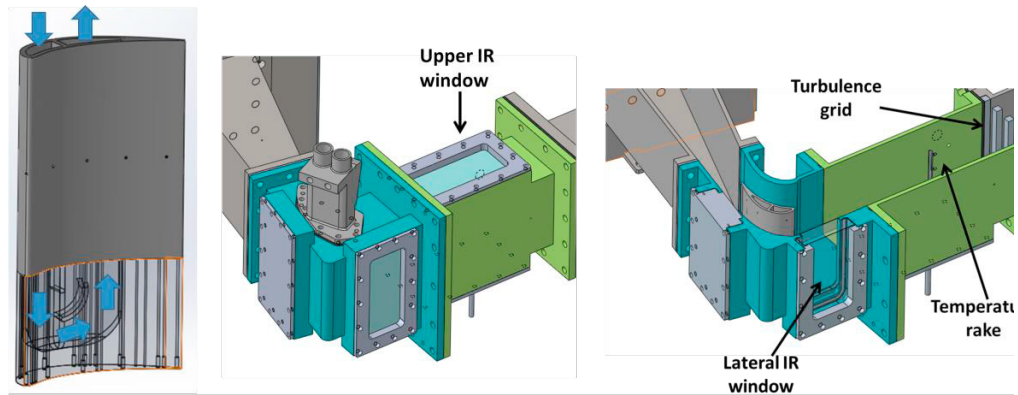


Fig. 1. 3D models of the test sample (a) and of the test section (b-c)

A turbulence grid placed about 5.5 axial chords upstream the blade leading edge is used to increase the turbulence intensity in the heated mainstream. The grid is made of parallel vertical square bars and has been designed using the approach suggested by Roach [12]; from hot wire anemometry measurements carried out 2.5 axial chords upstream the leading edge, a turbulence intensity of about 8.5%, is expected at the blade leading edge. A rake with five equally spaced thermocouples has also been used to evaluate the mainstream inlet total temperature and its profile. In nominal conditions, the temperature variation across the channel height was found to stay within 2.5 K.

Concerning optical accesses, rectangular 20 mm-thick potassium chloride (KCl) windows, shown in Fig. 1b and 2b, were used to acquire IR camera images. The first window is placed on the upper part of the inlet channel (Fig. 2a) and it allows to frame the bottom part of the blade Pressure side (PS). The second one is positioned on the side wall of the casing, to investigate the initial part of the blade suction side (SS) (Fig. 1c). A third optical access can be used to frame the final part of the blade SS, but it has not been used within this work.

## 2.2. Operating conditions

The operating conditions were chosen in order to match the values of the non-dimensional parameters that control the test rig behavior to relevant values, within the limits of the test facility; they are reported in Tab. 1.

Table 1. Operating conditions

Parameter	Value	Unit
Mainstream inlet Reynolds number	290000	-
Mainstream inlet Mach number	0.25	-
Expected throat Reynolds number	480000	-
Expected throat Mach number	0.65	-
Mainstream inlet temperature	600	K
Mainstream inlet total pressure	1.38	barA
Coolant Reynolds number	70000	-
Coolant Mach number	0.07	-
Mainstream-Coolant temperature ratio	2	-

Starting from these nominal conditions, coolant mass flow rate has been set to 100%, 200%, 300% and 400% of the nominal value, keeping unaltered its inlet pressure; mainstream mass flow rate was set to 100% and 50% of the nominal value. As a result, 8 different test conditions were explored.

### 3. Experimental results

Reduced optical accesses allow IR measurements to evaluate the blade temperature in the bottom part (non-dimensional blade height  $h/H_0$  lower than 50%) of the pressure side and on the first part (non-dimensional curvilinear abscissa  $s_{nd}$  lower than 23%) of the suction side. These areas are sketched in Fig. 2 and 3 with the respective results, expressed in terms of  $h/H_0$  and  $s_{nd}$ , thanks to an accurate image unwrapping procedure: marker points, at known blade span and abscissa, have been used to transform the acquired images into 2D maps.

Results are reported in Fig. 2 for the first camera position; maps are reported only for the extreme coolant mass flow rate conditions. A graph, showing the minimum temperature, measured in the investigated domain, has been used to show the temperature variation induced by the coolant for all the operating points. The position of the cooling channels has been reported on the figures as well. It is possible to recognize an area of high temperature close to the blade leading edge (LE), where both the mainstream adiabatic wall temperature and the external heat transfer coefficient are high, due to flow stagnation. Moving downstream the temperature decreases, since a reduction in external heat transfer coefficient is expected. A low-temperature area, clearly visible for test at nominal mainstream and coolant 400% and marked as A in the bottom right figure, can be seen in correspondence of position of the “cold” internal wall that separates the two cooling channels. A second low-temperature zone, marked as B, can be recognized close to the hub, in correspondence of the upward cooling channel, as the internal heat transfer coefficient is increased by the effect of the bend (C). For the test with reduced mainstream, zone B gets wider and zone A cannot be recognized anymore, even if, for coolant 400% test, the cold spot shape is such that it comprehends both zones. An increase in coolant mass flow rate, as shown by the top right plot, leads to a reduction in blade temperature, but, as expected, the entity of this reduction decreases in an asymptotic trend. Similarly, a reduction in mainstream mass flow rate brings to lower temperatures and such a decrease is more important, in absolute terms, for lower coolant mass flow rates.

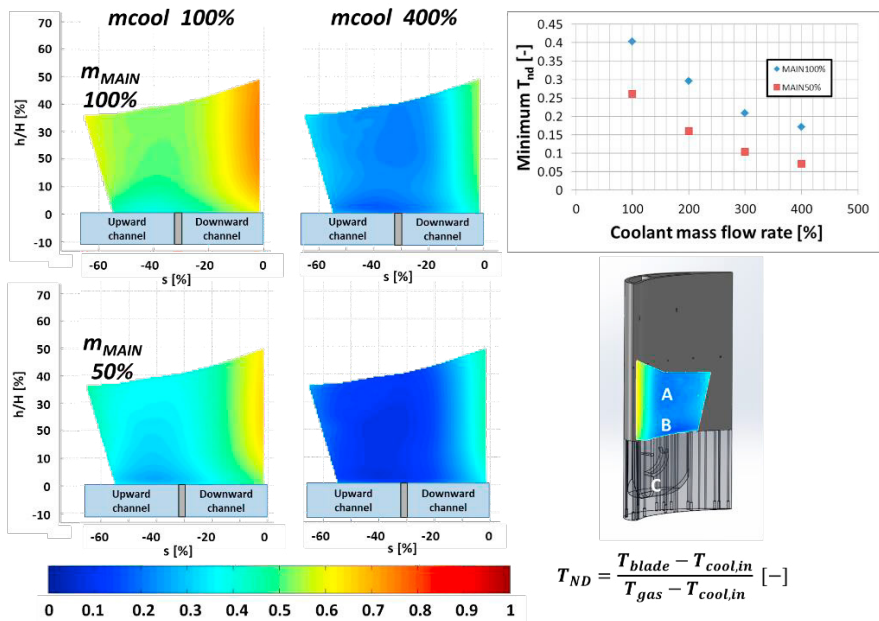


Fig. 2. Pressure side IR measurements

Fig. 3 shows the unwrapped images taken from the second IR camera position that visualizes the first part of the suction side, which is cooled only by the downward channel. In this area, the temperature field is markedly bi-dimensional and characterized by a decreasing metal temperature moving downstream. It is interesting to note that the minimum value is reached nearby the middle of the cooling channel ( $s_{nd} \approx 18-20\%$ ), way upstream than what happens on the pressure side. After that, a local increase is clearly visible, despite the proximity to the edge of the

investigated region. This phenomenon has been attributed to transition effects on the external flow path that leads to local external heat transfer enhancement. For tests with higher coolant mass flow rates (300% and 400%) it can be noted that the colder spot is not uniform, but it is rather divided into a two-points cold spot. In the authors’ opinion, this is due to two reasons: firstly, the cold zone at the tip is promoted by the lower coolant temperature, since it is progressively heated as it moves downstream; on the other hand, the internal heat transfer coefficient increases approaching the bend, resulting in the cold zone close to the hub. Similar considerations to the PS results can be taken regarding the minimum temperature trend, plotted in the top right plot.

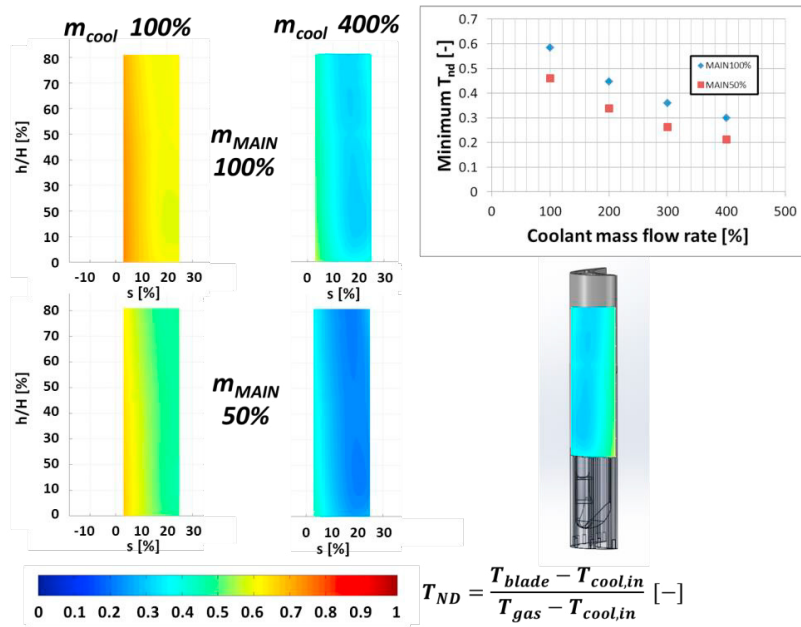


Fig. 3. Suction side IR measurements

#### 4. Numerical setup

Concerning the numerical validation of experimental results, analyses have been performed using the CFD solver ANSYS Fluent. The computational fluid domain used for the simulations is presented in Fig 4a.

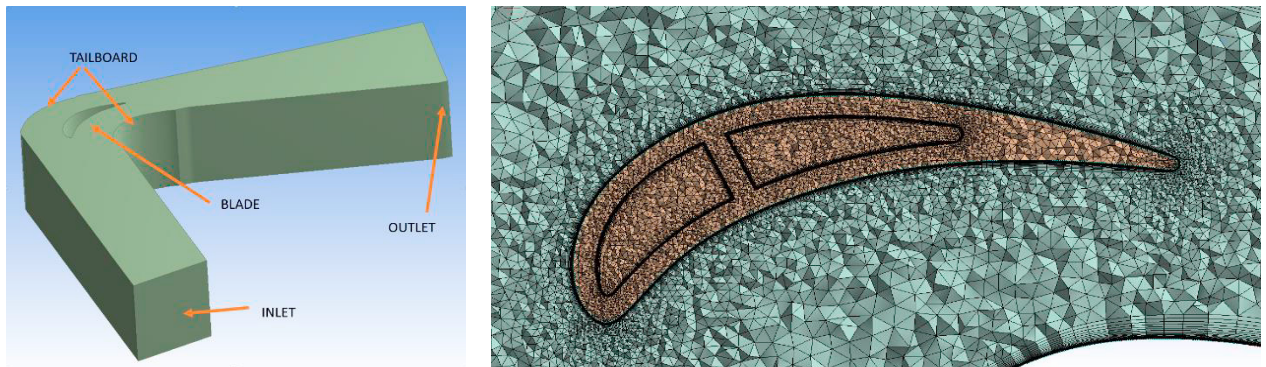


Fig. 4 - a) Computational domain b) Mesh details



Fig. 4b shows in details the mesh around the blade, including both internal and external fluid domains, as well as the blade. Including both fluid and solid regions is mandatory in order to perform a conjugate heat transfer analysis, for a total of 28M elements, of which 14M required only for the external flow path. Most of the elements are dedicate to provide an appropriate mesh for heat transfer simulation in presence of turbulent transition, i.e. with 25 inflation layers and a growth rate  $< 1.18$ ). Regarding the numerical setup, firstly, the objective is to find and validate the turbulence modelling strategy able to represent accurately experimental conditions. The configuration adopted is the one considering only the external flow path at 100%. Several turbulence models have been investigated and the results in terms of pressure distribution and heat transfer coefficient (HTC) are shown below. Turbulence models used for the analysis are the laminar model, the fully turbulent  $k-\omega$  SST, Langtry-Menter 4-equation transitional SST Model ( $\gamma-Re_{\theta t}$ ). Main flow 100% and coolant 100% case has been selected for the CHT simulations.

For the main flow simulation and for the CHT approach, adiabatic walls have been imposed everywhere, apart from the exterior surface of the vane. The first one has an imposed temperature, in the latter, the exterior and interior surface of the vane are coupled with their respective fluid part. For both cases, walls have been treated with a no-slip condition. The properties of air and metal have been characterized polynomial function of temperature.

## 5. Numerical results

### 5.1. External flow path results

Facchini et al. [11] showed that HTC profiles obtained without considering the transition, severely exceeded experimental data. Fig. 5a illustrates how accounting for transition, and turbulence in general, does not affect significantly the pressure distribution, overall returning a good agreement with experimental data. However, from Fig. 5b, it is clear how transition plays a key role in determining the HTC on the external surface of the blade. The prediction of the Transition SST model closely follows the trend exhibited by the laminar boundary layer in the very first part of the SS. After  $s_{nd} \approx 0.22$  the boundary layer shows a sudden transition to the conditions reproduced by the fully-turbulent model, which justify the metal temperature variation highlighted in Fig. 3. A different behavior is shown on the PS, where HTC values representative of turbulent conditions are returned in the proximity of the LE. However, the transition model highlights a laminarization process the gradually reduces heat transfer. Overall, it is worth underlining that different boundary layer conditions entail a significant increase in HTC values (more than a 100% from laminar to turbulent), pointing out the necessity to include a proper modelling of the transition process in the turbulence model. For these reasons, the 4 eq. transitional SST model has been adopted for the CHT analyses.

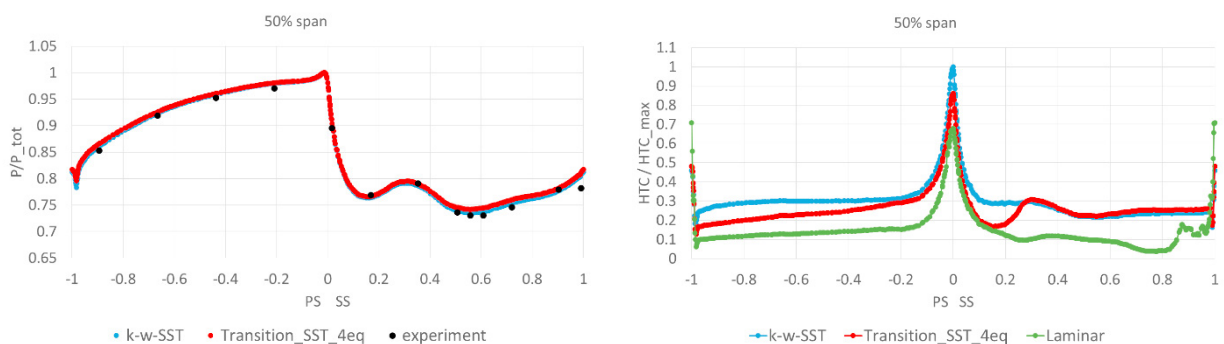


Fig. 5 - a) Pressure distribution b) HTC distribution

### 5.2. CHT results

The conjugate approach is able to predict the metal temperature distribution of the blade to perform a more comprehensive assessment of the experimental data. To allow a comparison against both thermocouples and IR measurements, only the span 20% is considered. A quantitative comparison of the metal temperature is reported in Fig. 6a, while Fig. 6b shows a qualitative trend of both metal temperature and velocity distribution.

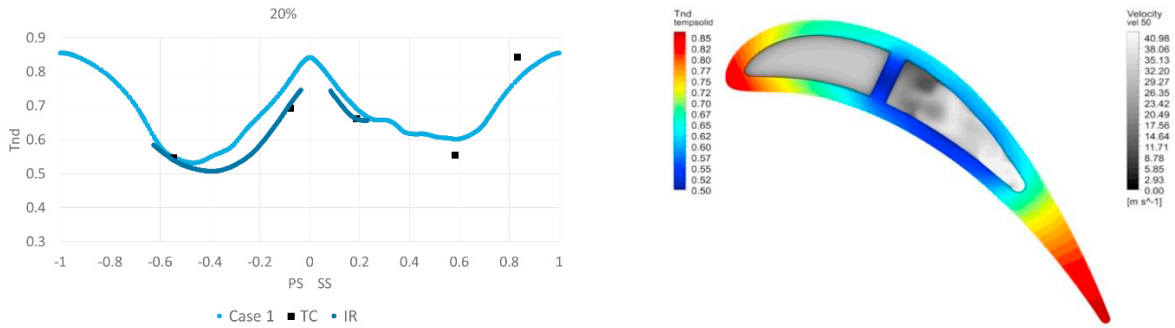


Fig. 6 - a)  $T_{nd}$  profile at 20% span, b) qualitative temperature and velocity distribution at 20% span

The central zone seems to act as a sink effect. The final part of the vane is deeply affected by heat transfer from the external fluid path since coolant channel stops at  $s_{nd} \approx 0.7$ . The downward channel at the LE features a relative non-turbulent flow, as compared to the upward channel, where a significant turbulence and mixing affect the results. Fig. 6a shows how, in the first half part of the vane, in the range  $-0.5 < s_{nd} < 0.5$ , simulations overestimate temperatures. This may be connected to the turbulence level of both external and internal fluid domains, as well as wall modelling. To better understand the problem, 3 cases have been analysed in addition to the reference Case 1. The results reported in Fig. 7a display how turbulence conditions of coolant have a marginal effect on the temperature (Case 2 and 3). On the other hand, a mainstream turbulence intensity reduced of 2.1% (Case 4) succeeds in decreasing metal temperature.

Table 2 - Numerical test boundary conditions

	Tu Probe (%)	Tu LE (%)	Length main (mm)	Tu coolant (%)	Length coolant (mm)
<b>Case 1</b>	10.1	8.3	4.38	10	3
<b>Case 2</b>	10.1	8.3	4.38	20	3
<b>Case 3</b>	10.1	8.3	4.38	10	6
<b>Case 4</b>	8	5.9	4.38	10	3

It is also worth considering the impact of roughness on heat transfer. The additive manufacturing technique entails a roughness of  $50 \mu m$  on the cooling channels (while the external surface is painted to perform IR measurements). An additional simulation has been performed with the nominal boundary conditions, but exploiting a rough wall formulation. It can be observed in Fig. 7b that the zone interested by the cavity experiences a sensible reduction in temperature. The closer to the trailing edge, the lower this reduction: the zone close to the trailing edge is barely affected by internal cooling, therefore its temperature mostly relies on the external flow path conditions.

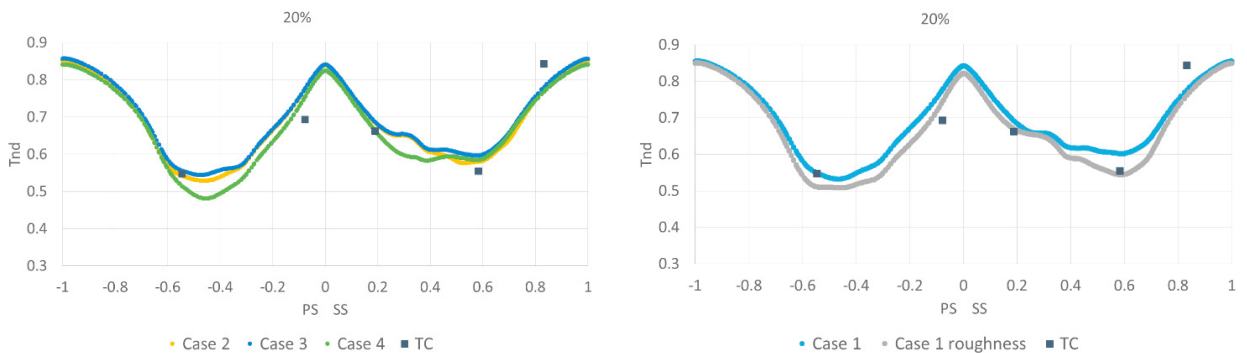


Fig. 7 - a) Sensitivity to turbulence conditions on  $T_{nd}$ , b) Sensitivity to roughness on  $T_{nd}$

## 6. Conclusions

The combined use of IR measurements and CHT approach gives a deep insight into the heat transfer mechanisms determining metal temperature. In the very first part of the SS, the temperature field is markedly 2D and determined by the progressive thickening the laminar boundary layer followed by a sudden transition to turbulent conditions. On the other hand, the HTC trend on the PS is rather uniform, therefore the temperature pattern results more influenced by the characteristics of the internal cooling system. In general, the increase in the cooling flow and the reduction of the mainstream lead to a reduction of the metal temperature, even though this process becomes progressively less efficient the coolant flow is increased.

Numerical results have proved the robustness of the  $\gamma$ - $Re_{ot}$  transition model. Sensitivity analyses have shown the more relevant role of mainstream turbulence condition on the resulting metal temperature as compared to the internal side. An equally important role seems to be played by wall roughness, which can substantially enhance heat transfer in absence of other turbulence promoters such as ribs or pin fins.

## Acknowledgments

The authors would like to express their gratitude to Ansaldo Energia for the permission to publish this work.

The valuable contribution given by Prof. Bruno Facchini during the experimental campaign is also acknowledged.

## References

- [1] Ho K.S., Liu J.S., Elliott T. and Aguilar B. "Conjugate heat transfer analysis for gas turbine film-cooled blade" *ASME Paper GT2016-56688*, (2016).
- [2] Hylton L. D., Mihelc M. S., Turner E. R., Nealy D. A. and York R. E. "Analytical and experimental evaluation of the heat transfer distribution over the surfaces of turbine vanes." *NASA Contractor Report, NASA CR-168015*, (1983).
- [3] Han J.-C., Dutta S. and Ekkad S.V "Gas Turbine Heat Transfer and Cooling Technology" 2<sup>nd</sup> edition, Taylor&Francis (2013)
- [4] Ekkad S.V., Ou S. and Rivir R.B. "A transient infrared thermography method for simultaneous film effectiveness and heat transfer coefficient measurements from a single test." *Journal of Turbomachinery*, 126, pp.597–603, (2004).
- [5] Lynch S. and Thole K. "The effect of combustor-turbine interface gap leakage on the endwall heat transfer for a nozzle guide vane." *ASME Paper GT2007-27867*, (2017).
- [6] Cocchi L., Facchini B., Giuntini S., Winchler L., Tarchi L., Innocenti L., Andrei L. and Bonini A. "Experimental investigation on impingement array cooling systems through IR thermography" *ASME Paper GT2016-57436*, (2016).
- [7] Goodro M., Park J., Ligrani P., Fox M. and Moon H.-K. "Effects of mach number and reynolds number on jet array impingement heat transfer". *International Journal of Heat and Mass Transfer*, 50(1), pp. 367–380, (2007).
- [8] Carlomagno G. M. and Cardone G. "Infrared thermography for convective heat transfer measurements" *Experiments in fluids*, 49(6), (2010).
- [9] Bohn D. E., Bonhoff B. and Schonenborn H. "Combined Aerodynamic and Thermal Analysis of a Turbine Nozzle Guide Vane," *IGTC Paper 95-108*. (2005).
- [10] York W. D. and Leyle J. H. "Three-Dimensional Conjugate Heat Transfer Simulation of an Internally-Cooled Gas Turbine Vane", *ASME paper GT2003-38551*, (2003).
- [11] Facchini B., Magi A. and Greco A., S. "Conjugate Heat Transfer of a Radially Cooled Gas Turbine Vane," *ASME paper GT2004-54213*, (2004).
- [12] Andrei L., Andreini A., Facchini B. and Winchler L. "A decoupled CHT procedure: application and validation on a gas turbine vane with different cooling configurations" *Energy Procedia*, 45, pp. 1087–1096, (2014).
- [13] Roach P.E. (1987) "The generation of nearly isotropic turbulence by means of grids." *International Journal of Heat and Fluid Flow* 8.2 (1987).